ISSN (Print) 1226-1750
ISSN (Online) 2233-6656
Journal of Magnetics 24(3), 448-453 (2019) https://doi.org/10.4283/JMAG.2019.24.3.448

A Non-Linear Permanent Magnet Working Point Migration Model and its Application to Simulation of a Polarized Magnetic System

Bo Li[1], Huimin Liang[1], Jiaxin You[1]*, Fangyuan Xiong[1], and Jan K. Sykulski[2]

[1]Department of Electrical Engineering, Harbin Institute of Technology, Harbin 150001, China
[2]School of Electronics and Computer Science, University of Southampton, Southampton, SO17 1BJ, UK

(Received 20 July 2018, Received in final form 29 August 2019, Accepted 29 August 2019)

The paper addresses the issue of the working point migration in non-linear permanent magnets (PM). Starting from the considerations of energy, a novel working-point migration (WPM) model is proposed which can be incorporated into a magnetic equivalent circuit (MEC). The basic theory of working-point migration is discussed which focus on the second quadrant of the magnetic hysteresis loop. The calculation method of the WPM model is proposed based on the relationship between the recoil line model and the affine transformation hysteresis loop. The establishment method for the resultant working point is described by combining the demagnetization curve and the recoil line models in the minor hysteresis loop. The static characteristic of a bistable polarized magnetic system (BPMS), as used in actuators, is calculated using the magnetic circuit method based on the WPM, while a finite element model (FEM) is also derived. The calculation method for the WPM used in MEC is also discussed. The WPM based MEC model yields reasonable results, compared with FEM, of the latching force but with much faster calculation speeds. Furthermore, the working-point state of the PM is clearly illustrated. The test system of the BPMS prototype is established. The test data and WPM model calculation results are compared. It is shown that the WPM model provides accurate prediction of static characteristics of an electromagnetic system.

Keywords : nonlinear permanent magnet, operation point, hysteresis model, magnetic equivalent circuit, bistable polarized magnetic system

1. Introduction

Nonlinear permanent magnet such as AlNiCo is widely used in polarized magnetic systems due to its stable structure, high Curie point, simply manufactural and low cost. However, it has the phenomenon of working point migration (WPM). Even demagnetization may occur under special conditions (e.g. coil overload). The phenomenon is quite complex and there is only few reliable simulation methods.

Some research have been made to address such WPM issue. An inverse hysteresis model based on spline approximation [1] achieves good accuracy only the calculation may be a little bit cumbersome. The working point in PM may express the change of the performance, even the demagnetization process [2]. A linear approximate hysteresis model of AlNiCo [3] allows transient calculation of a permanent magnet (PM) motor although the model is somewhat inflexible. A hysteresis model [4] based on a support vector machine (SVM) approach uses statistical learning theory and structural risk minimization principle, which may require significant amount of test data and must allow time for training. A temperature dependent hysteresis model [5] based on a vector-play model (VPM) was also proposed, but the mathematical derivation of the model is a little bit complex. PM working point based model is attempted to simply calculate the flux density for an actuator [6].

At the same time it is recognized that the WPM phenomenon is an important issue and has a direct impact on the performance of electrical machines and actuators. Examples of recent studies include research on the effects of irreversible demagnetization on the characteristics of a brushless direct current motor (BLDC) [7, 8], investigation of the relationship between rotor geometry and irreversible demagnetization using FEM models [9]; and temperature effects and the influence of short-circuit current on permanent magnets [10]. Although the work-

*Corresponding author: Tel: +86-0451-86413193
Fax: +86-0451-86413964, e-mail: ibic2013@126.com

ing points based model can not calculate maximum torque per ampere or flux weakening characteristics which cannot be targeted directly on the FEM tool [11], it is also very important for optimization design process [12, 13].

Based on some work before [14, 15], a WPM model of a non-linear PM exploiting the affine transformation is established. The working principle of the WPM model is first established and explained, followed by the description of the solution process. For illustrative purposes the WPM model is applied to the calculation of the static characteristic of a polarized magnetic system. The magnetic equivalent circuit (MEC) representation based on the WPM model is derived to facilitate the calculation. In order to verify the proposed modelling methodology a prototype actuator has been manufactured and static characteristics measured, with some details of the testing rig provided. The results show that the WPM approach proposed in this paper is capable of describing the WPM phenomenon while the MEC model has high accuracy and good computational efficiency.

2. The Working Point Migration Model

A non-linear working-point migration (WPM) model – based on the affine transformation method – is established relying on a demagnetization curve representation, the recoil line model and the affine transformation hysteresis loop model, all shown in Fig. 1.

The initial working point is located at Q_0 in Fig. 1 and the working point migration process can be described using the demagnetization curve model shown by the black line. If, after demagnetizing, the working point migrates to Q_1, then a new working point – when magnetized again – will follow the recoil line shown by the green line.

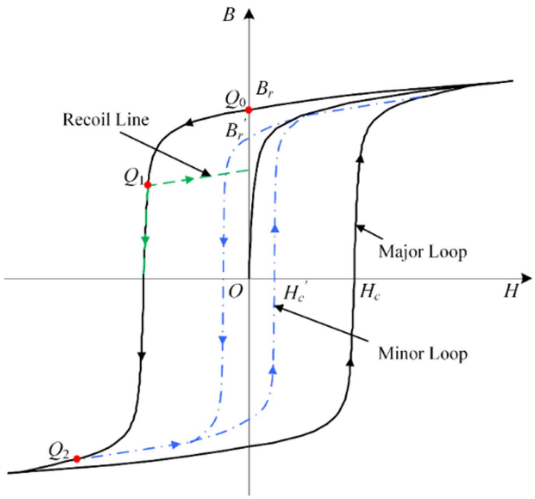

Fig. 1. (Color online) The working point migration process.

To establish a simple calculation model the affine transformation method is used to build the WPM model. If the top point $Q(x_m,y_m)$ of a small hysteresis loop is set to coincide with the top point of the main hysteresis loop $Q_2(x_{m2},y_{m2})$, then we can write

$$\begin{bmatrix} x_{m2} \\ y_{m2} \\ 1 \end{bmatrix} = \mathbf{A} \begin{bmatrix} x_m \\ y_m \\ 1 \end{bmatrix} = \begin{bmatrix} \alpha_{11} & \alpha_{12} & u_x \\ \alpha_{21} & \alpha_{22} & u_y \\ 0 & 0 & 1 \end{bmatrix} \begin{bmatrix} x_m \\ y_m \\ 1 \end{bmatrix} \tag{1}$$

where **A** is a transformation matrix specifying the enlargement range between the small hysteresis loop and the main hysteresis loop. A simple affine transformation form may be used

$$\begin{bmatrix} x_{m2} \\ y_{m2} \\ 1 \end{bmatrix} = \begin{bmatrix} \alpha_1 & 0 & 0 \\ 0 & \alpha_2 & 0 \\ 0 & 0 & 1 \end{bmatrix} \begin{bmatrix} x_m \\ y_m \\ 1 \end{bmatrix} \tag{2}$$

where α_1 and α_2 represent the 'zooming factors' from the main hysteresis loop to the small hysteresis loop following the affine transformation. The inverse transformation can be deduced as

$$\begin{bmatrix} x_m \\ y_m \\ 1 \end{bmatrix} = \begin{bmatrix} \beta_1 & 0 & 0 \\ 0 & \beta_2 & 0 \\ 0 & 0 & 1 \end{bmatrix} \begin{bmatrix} x_{m2} \\ y_{m2} \\ 1 \end{bmatrix} = \begin{bmatrix} 1/\alpha_1 & 0 & 0 \\ 0 & 1/\alpha_2 & 0 \\ 0 & 0 & 1 \end{bmatrix} \begin{bmatrix} x_{m2} \\ y_{m2} \\ 1 \end{bmatrix} \tag{3}$$

with

$$\begin{cases} x_{m2} = x_m / \alpha_1 \\ y_{m2} = y_m / \alpha_2 \end{cases} \tag{4}$$

By combining the demagnetization curve and the recoil line models in the minor hysteresis loop, the resultant working point can be established. In the small loop, the working point will move ion the same way as in the main hysteresis loop.

3. Application of the WPM Model to a Polarized Magnetic System

A typical bistable polarized magnetic system (BPMS) is used to illustrate the methodology; it consist of a solenoid actuator with permanent magnets. Such devices may be used in high voltage contactors and actuators. The structure of the system is shown in Fig. 2, where the PM in the top layer is made from AlNiCo and in the lower layer from NdFeB. The soft magnetic components are made of DT4E. The soft magnet parts and air gap is clearly showed in the structure.

The working principle of the BPMS is described graphically with the black and red dashed lines depicting

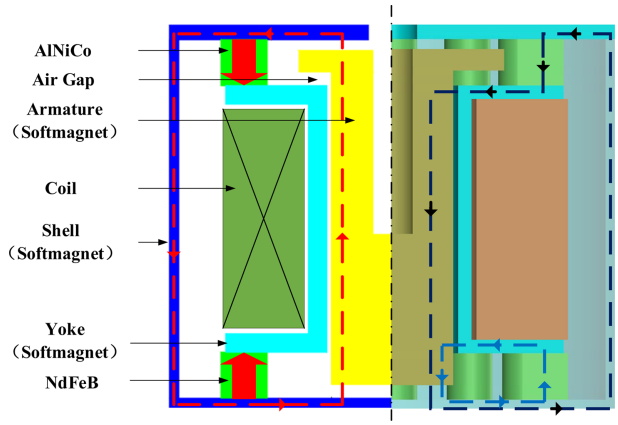

Fig. 2. (Color online) The structure of the BPMS.

the magnetic flux of the magnets and the electromagnet, respectively. With the coil excited for forward movement, the fluxes due to the PM and the electromagnet are in opposition in the lower air gap, which results in a decrease of the downward magnetic force.

In the upper air gap, on the other hand, the two fluxes act in the same direction resulting in an increase of the upward force. Consequently, the armature is pulled up by the upward net force. Conversely, with a reverse coil current, the armature is pulled down by the downward force. The flux paths related to different states are shown in Fig. 3.

The equivalent magnetic circuit is established in combination with the WPM model. The describing equations of the magnetic equivalent circuit model are

$$\begin{cases} F_1 = (R_{ma12} + R_{mg1} + R_{ms1} + R_{mc1})\Phi_1 - R_{mc1}\Phi_2 \\ F_2 = R_{mc2}\Phi_2 - (R_{ma22} + R_{mg2} + R_{ms2} + R_{mc2})\Phi_3 \\ NI = -(R_{ma12} + R_{mg1} + R_{ms1})\Phi_1 - (R_{ma11} + R_{ms3} + R_{ma21}) \\ \Phi_2 - (R_{ma22} + R_{mg2} + R_{ms2})\Phi_3 \end{cases} \tag{5}$$

Applying the WPM model yields the equivalent magnetic circuit of Fig. 4. Using the WPM model and the previous (or initial) working point, a temporary working point is found as

$$\begin{cases} H_1 = F_1 / l_1 \quad H_2 = F_2 / l_2 \\ B_1 = (\Phi_1 - \Phi_2) / S_1 \\ B_2 = (\Phi_2 - \Phi_3) / S_2 \\ B_1 = f_1(H_1) \quad B_2 = f_2(H_2) \end{cases} \tag{6}$$

where f_1 and f_2 represent the WPM model of the upper layer AlNiCo and the lower layer NdFeB, respectively, while Φ_1 and Φ_2 represent the branch magnetic fluxes of the upper air gap and the lower air gap, respectively.

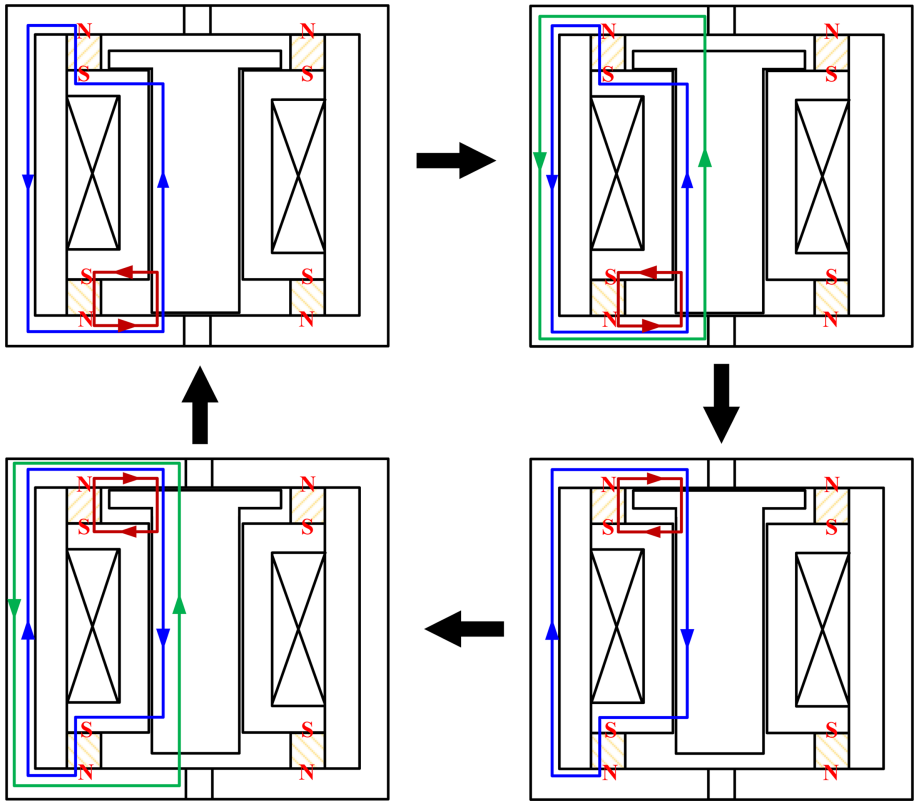

Fig. 3. (Color online) The flux paths for the BPMS in different states.

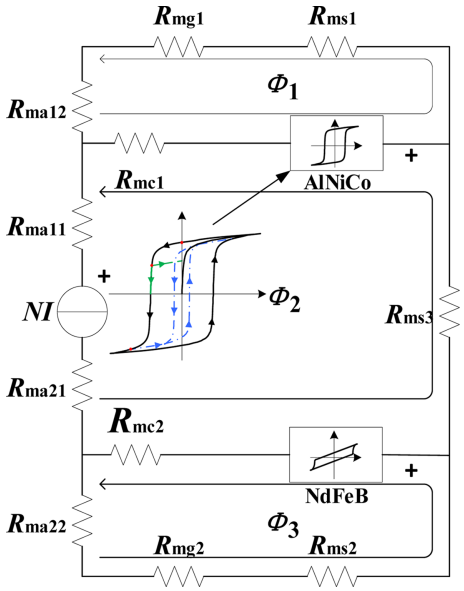

Fig. 4. (Color online) The MEC model of the BPMS.

The temporary PM working point is thus calculated. Then the magnetomotive forces (*mmf*) and branch fluxes are calculated using the magnetic equivalent circuit. The main MEC model for the BPMS considered is shown in Fig. 4.

The solution process for the proposed methodology can be divided into several stages, as depicted in Fig. 5. Compared with the sequence used to create the MEC model, there is an additional iteration.

First, the initial value of the PM working point is set for the WPM model. From the WPM model, the *mmf* of the MEC can be calculated. Then the MEC functions (5) are solved iteratively (e.g. using the Newton-Raphson method), from which the fluxes can be found. Furthermore, the current working point can be calculated. If this point 'outside' the PM matches the working point in the WPM model, the working point in the WPM model is updated; otherwise, the working point of the WPM model can be renewed iteratively and the above process is repeated.

In this process, the temporary PM working point is fixed according to the WPM model and the branch magnetic fluxes. The computation is repeated iteratively until the final position of the working point and the resultant force can be calculated.

4. Comparison between Test and Calculation Results

4.1. The BPMS prototype

The prototype BPMS is shown in Fig. 6. To test the dynamic force of the BPMS, the two static and one moveable contacts are connected with an outer armature. In this prototype, the initial state of the 24 PMs (12 AlNiCo and 12 NdFeB) is that they are all fully magnetized.

4.2. The test rig for the BPMS

The schematic of the test rig presents in Fig. 7. The force measurement was relatively straightforward but the position of the working point could only be established indirectly. Two measurements are involved independently, the magnetic field strength on the surface of the magnet and the total magnetic flux in a 'section' using a specially

(a) The prototype BPMS (b) CAD model

Fig. 6. (Color online) The BPMS prototype (shown without the armature).

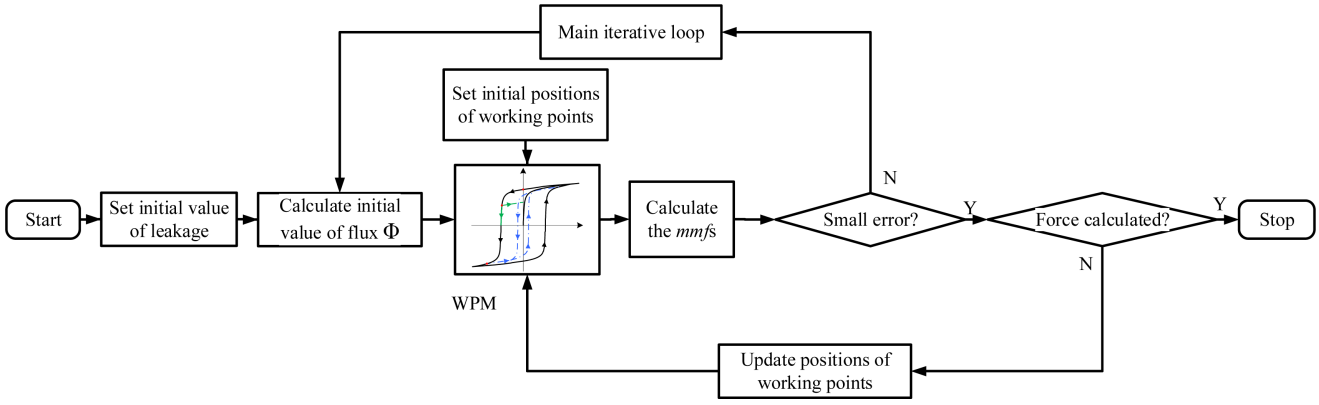

Fig. 5. (Color online) The solution process for the MEC combined with the WPM model.

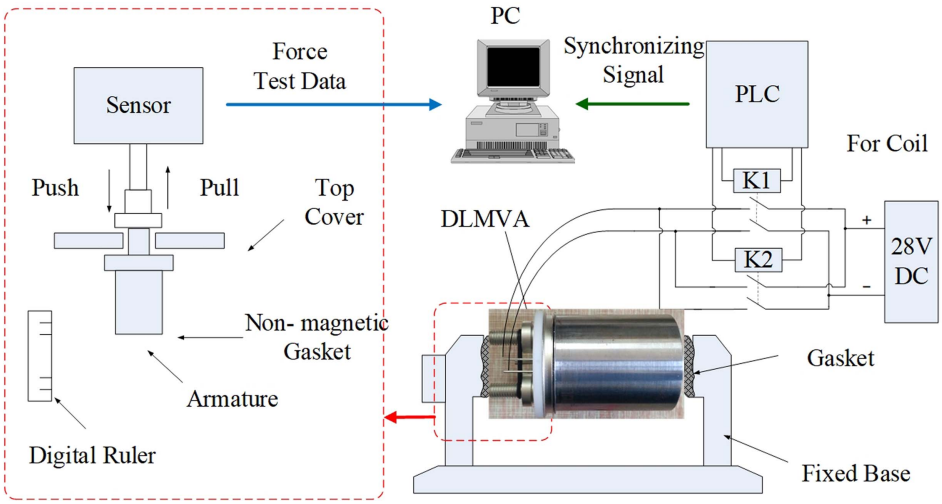

Fig. 7. (Color online) The BPMS prototype force test rig.

wound coil. From the practical point of view, two aspects of the experiment are very important: the verticality of the force test block and the concentricity of the section flux test coil.

4.3. Test results and the comparison

The measured and calculated values are shown in Fig. 8 as a function of the coil ampere-turns. For the permanent magnets in different layer, the move tracks are the same. For the surface flux density, the results from a finite element method (FEM) are included, showing the inability of this method to capture the important effect. Overall, the simulation results using the MEC model can satisfy the experiment data well.

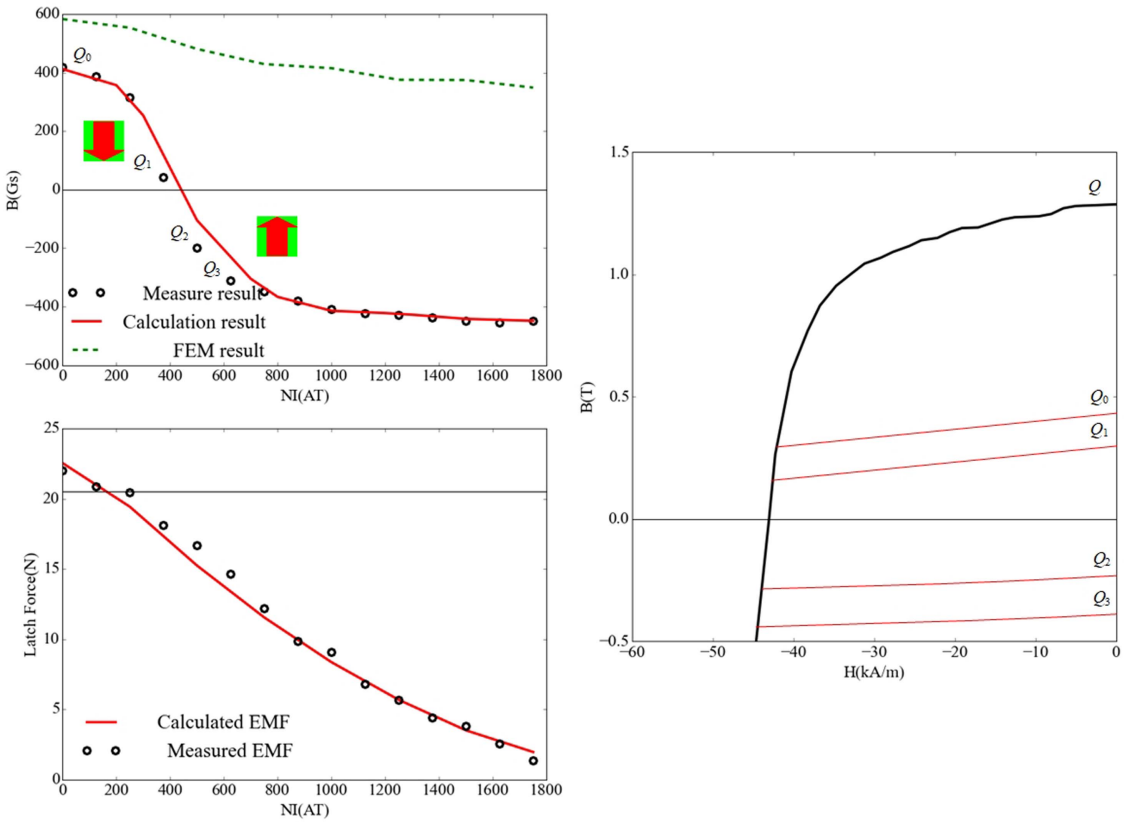

Fig. 8. (Color online) Measured and calculated results for the surface flux density (top left) and the latching force (bottom left) as a function of the ampere-turns. The graph on the right shows the recoil lines for the four selected values.

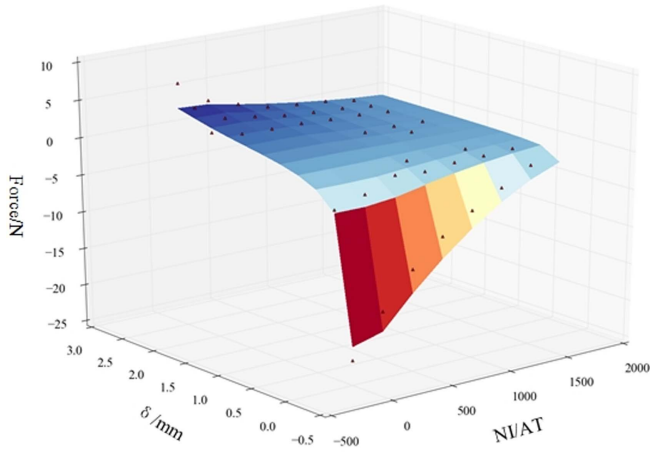

Fig. 9. (Color online) Measured (dot line) and calculated results for the upper PM.

It is worth noting that from the value of the ampere-turns of about 500A the magnetic field changes into reverse direction. The PM can reach a reverse saturation point above 12000A.

Fig. 9 shows the calculated and measured latching force results for the extended values of the air-gap and ampere-turns. The agreement is very pleasing indeed, with an average error of about 9.8 %. The biggest discrepancies occur in the low voltage region, where – on one hand – it is hard to maintain the accuracy of the hysteresis loop model, and – at the same time – the measurements of very low values may be unreliable. Finally, it is worth noting that on average it takes about 1.5 s to compute one point using the MEC, whereas for the FEM the required time is 270 s, thus the savings in simulation time are significant.

5. Conclusions

Based on the fundamental relationships pertaining to the hysteresis loop description, a working-point migration model for permanent magnets has been developed. The solution procedure is also proposed. It has been demonstrated that the magnetic circuit representation based on the working-point migration model put forward enables accurate and very fast calculations of the performance – in particular the magnetic force – of a BPMS. Thanks to reasonable accuracy and very short computing times, this proposed model can therefore be used for analysis and robust design optimization.

Acknowledgement

This paper is supported by NSFC (National Natural Science Foundation of China) Project 51507033, 51707044 and China Postdoctoral Science Foundation 2016M591530.

References

[1] S. E. Zirka, Y. I. Moroz, R. G. Harrison, and N. Chiesa, IEEE Trans. Power Delivery, **29**, 552 (2014).
[2] T. A. Huyunh and Min-FuS Hsieh, IEEE Trans. Magn, **55**, 99 (2019).
[3] C. Yu, S. Niu, S. L. Ho, W. Fu, and L. Li, IEEE Trans. Magn. **51**, 1 (2015).
[4] S. Zhang, M. Wang, P. Zheng, G. Qiao, F. Liu, and L. Gan, IEEE Trans. Magn. **53**, 1 (2017).
[5] A. Bergqvist, D. Lin, and P. Zhou, IEEE Trans. Magn. **50**, 345 (2014).
[6] Mingqiao Wang, Chengde Tong, P. Zheng, L. Cheng S. Zhang, G. Qiao, and Y. Sui, IEEE Trans. Magn. **55**, 207 (2019).
[7] J. H. Park, H. K. Kim, S. T. Lee, and J. Hur, Proceedings of the 2016 IEEE Conf. Electromagnetic Field Computation (2016).
[8] H. K. Kim and J. Hur, IEEE Trans. Ind. Appl. **53**, 982 (2017).
[9] L. Guo, C. Xia, and Z. Wang, Proceedings of the 2017 IEEE International Magnetics Conf. (2017).
[10] G. J. Li, P. Taras, Z. Q. Zhu, J. Ojeda, and M. Gabsi, IET Electric Power Appl. **11**, 595 (2017).
[11] C. A. Rivera, J. Poza, G. Ugalde, and G. Almandoz, Energies **11**, 1288 (2018).
[12] J. Linden, Y. Nikulshin, A. Friedman, Y. Yeshurun, and S. Wolfus, Energies **12**, 1823 (2019).
[13] Jae Suk Lee, Energies **11**, 2027 (2018).
[14] H. M. Liang, J. You, W. Y. Yang, and G. F. Zhai, J. Magn. **19**, 32 (2014).
[15] J. You, K. Zhang, Z. W. Zhu, and H. M. Liang, J. Magn. **21**, 65 (2016).